

## Measuring biological age in mice using differential mass spectrometry

Harris Bell-Temin<sup>1</sup>, Matthew J. Yousefzadeh<sup>2,3</sup>, Andrey Bondarenko<sup>4</sup>, Ellen Quarles<sup>5</sup>, Jacqueline Jones-Laughner<sup>6</sup>, Paul D. Robbins<sup>2,3</sup>, Warren Ladiges<sup>7</sup>, Laura J. Niedernhofer<sup>2,3</sup>, Nathan A. Yates<sup>1,6</sup>

<sup>1</sup>Department of Cell Biology, University of Pittsburgh School of Medicine, Pittsburgh, PA 15261, USA

<sup>2</sup>Department of Molecular Medicine, The Scripps Research Institute, Florida, Jupiter, FL 33458, USA

<sup>3</sup>Department of Biochemistry, Molecular Biology and Biophysics, and the Institute on the Biology of Aging and Metabolism, University of Minnesota, Minneapolis, MN 55455, USA

<sup>4</sup>Infoclinika, Bellevue, WA 98006, USA

<sup>5</sup>Department of Pathology, University of Washington, Seattle, WA 98195, USA

<sup>6</sup>Biomedical Mass Spectrometry Center, University of Pittsburgh Schools of the Health Sciences, Pittsburgh, PA 15261, USA

<sup>7</sup>Department of Comparative Medicine, School of Medicine, University of Washington, Seattle, WA 98195, USA

**Correspondence to:** Nathan A. Yates, Laura J. Niedernhofer; **email:** [yatesn@pitt.edu](mailto:yatesn@pitt.edu), [lniedern@unm.edu](mailto:lniedern@unm.edu)

**Keywords:** proteomics, non-targeted, surrogate markers, aging, mouse, liver, mass spectrometry

**Received:** January 14, 2019

**Accepted:** January 29, 2019

**Published:** February 11, 2019

**Copyright:** Bell-Temin et al. This is an open-access article distributed under the terms of the Creative Commons Attribution License (CC BY 3.0), which permits unrestricted use, distribution, and reproduction in any medium, provided the original author and source are credited.

### ABSTRACT

Aging is an ill-defined process that increases the risk of morbidity and mortality. Aging is also heterogeneous meaning that biological and chronological age can differ. Here, we used unbiased differential mass spectrometry to quantify thousands of proteins in mouse liver and select those that consistently change in expression as mice age. A panel of 14 proteins from inbred C57BL/6 mice was used to equate chronological and biological age in this reference population, against which other mice could be compared. This “biological age calculator” identified two strains of f1 hybrid mice as biologically younger than inbred mice and progeroid mice as being biologically older. In an independent validation experiment, the calculator identified mice treated with rapamycin, known to extend lifespan of mice, as 18% younger than mice fed a placebo diet. This demonstrates that it is possible to measure subtle changes in biologic age in mammals using a proteomics approach.

### INTRODUCTION

Aging is the greatest risk factor for the majority of chronic diseases. The world’s population is rapidly aging with the number of individuals over 65 estimated to double by 2050 [1]. More than 90% of adults over 65 have at least one chronic disease, and over two-thirds have two or more, accounting for >70% of deaths in America and 95% of all healthcare costs for the elderly [2]. Recently, efforts were initiated to begin therapeutically targeting aging with the goal of simultaneously delaying the onset of multiple chronic diseases [3, 4]. The development of new treatments for aging will depend greatly on the identification of biomarkers

that act as surrogates for measuring lifespan and healthspan, which are costly and lengthy to measure in pre-clinical models, let alone in humans [5].

Several hurdles complicate the discovery and development of molecular biomarkers of aging. This includes the time required to age animals, the need to test large numbers of candidate markers, and the translation of tests between models and species. Proteomic approaches offer attractive solutions to these challenges and hold great potential for identifying protein profiles that can serve as surrogate markers of “biological age”. First, mass-spectrometry based measures can examine thousands of candidate proteins from archived tissues

and bio-fluids, thus economically enabling discovery of new biomarkers. Second, proteomic measures facilitate analysis of numerous strains of mice, genetic models of aging and treatment groups relative to a reference population, to accelerate testing and validation of biomarkers. Finally, mass spectrometry assays are based on the chemical measurement of specific amino acid sequences, not biological antibody recognition, thus allowing proteins to be tested across species with absolute molecular specificity.

Aging in most species is tremendously heterogeneous at both the organismal and molecular level [6, 7]. As a result, precise measurements and sufficiently large sample sizes are needed to detect subtle, yet reproducible, changes in protein expression that occur as organisms age. In fact, a previous study using unbiased proteomics to detect global protein expression changes in mouse tissues that occur with aging yielded only 5 proteins, using a cut-off of 2-fold change in expression [8]. In a similar study on rat heart, the greatest differential in age-related protein expression changes was 2-fold [9]. Hence approaches are needed that enable detection of more subtle changes in protein expression.

Here, we took an unbiased proteomics approach to measure differences in protein expression in the livers of mice with aging. We chose to focus on liver because of the technical challenges associated with the large dynamic range ( $\sim 10^{10}$ ) of protein concentrations in plasma [10]. One unique feature of our approach was that rather than a binary design (old vs. young), we analyzed at least 4 age groups over the lifespan of mice to identify changes in protein expression that occur with aging. A second unique feature of our approach was the analysis of a large number of samples ( $n=7-8$  mice per age, sex, strain), which is only possible when using a label-free method of protein detection. The third unique feature was to utilize a differential mass spectrometry (dMS) workflow that prioritizes global protein quantification over identification (see [11-13] and Supplementary Figure 1 for details). This yields a molecular profile with hundreds of thousands of signals per liver that can be analyzed for age-related signatures and readily identified by amino acid sequence in follow-up analyses. The large sample size, multifactorial experimental design and emphasis on precise quantification greatly enhanced our ability to identify robust molecular features that exhibit a statistically significant yet subtle difference in expression between age groups. Finally, in a separate experiment performed nine months after the initial discovery study and utilizing liver samples obtained from an independent investigator/institution, we confirmed that the aging protein expression profile could be reproduced and used to detect a reduction in

biological age induced by a drug intervention known to extend the lifespan of mice.

## RESULTS

The experimental design is illustrated in Figure 1. Male C57BL/6Jnia (inbred) mice were used as the reference population and compared to male mice in an f1 hybrid background (C57BL/6Jnia:Balb/cBy; called f1a) and female mice in a second f1 background (C57BL/6J:FVB/NJ; called f1b) (Figure 1A). The identities of the liver samples were blinded and a balanced incomplete block design (see methods for details) was used to minimize the impact of order bias that can be introduced during sample processing and analysis. Error introduced during sample processing and analysis was determined from the analysis of technical replicate samples from a pooled control. Sample preparation was carried out in parallel using a block size of 48 samples and then individual samples were analyzed sequentially by nano-flow liquid chromatography high-resolution mass spectrometry (nLC-MS). This label-free dMS workflow supports the unbiased quantification of proteomic features over the large number of samples required for this multilevel analysis (Figure 1B). Supplementary Table 1 lists all samples processed simultaneously in the initial discovery experiment ( $n=140$  liver samples).

A cloud-computing dMS analysis pipeline (Infoclinika, Bellevue, WA) that enables the analysis of large nLC-MS data sets was used to detect and quantify levels upwards of a hundred thousand high resolution features per liver lysate. A data-cube structure was used to store the full dataset and enhance computationally intensive feature alignment and quantification calculations. Each feature is defined by its mass-to-charge ratio ( $m/z$ ) and retention time ( $rt$ ). The feature intensity ( $i$ ) provided a relative measure of protein expression that can be compared across samples. Features that exhibited large fluctuations in intensity were removed from the dataset using occupancy filtering (features that appeared in  $<4$  mice per strain/sex/age group) and outlier removal criteria (features that were greater than one order of magnitude outside the group median intensity level). Volcano plots of statistically significant features showed a similar number of features with increased or decreased expression with age (Figure 1C). Features linked to a common protein sequence were combined to yield protein-level expression data. More details on data analysis are provided in Supplementary Figure 1. It is important to note that differences in protein expression ( $x$ -axis, Figure 1C) were subtle ( $<1$ -fold increase) for the majority of proteins, illustrating why previous proteomic studies that used fewer numbers of samples failed to detect these differences as statistically significant [8, 14].

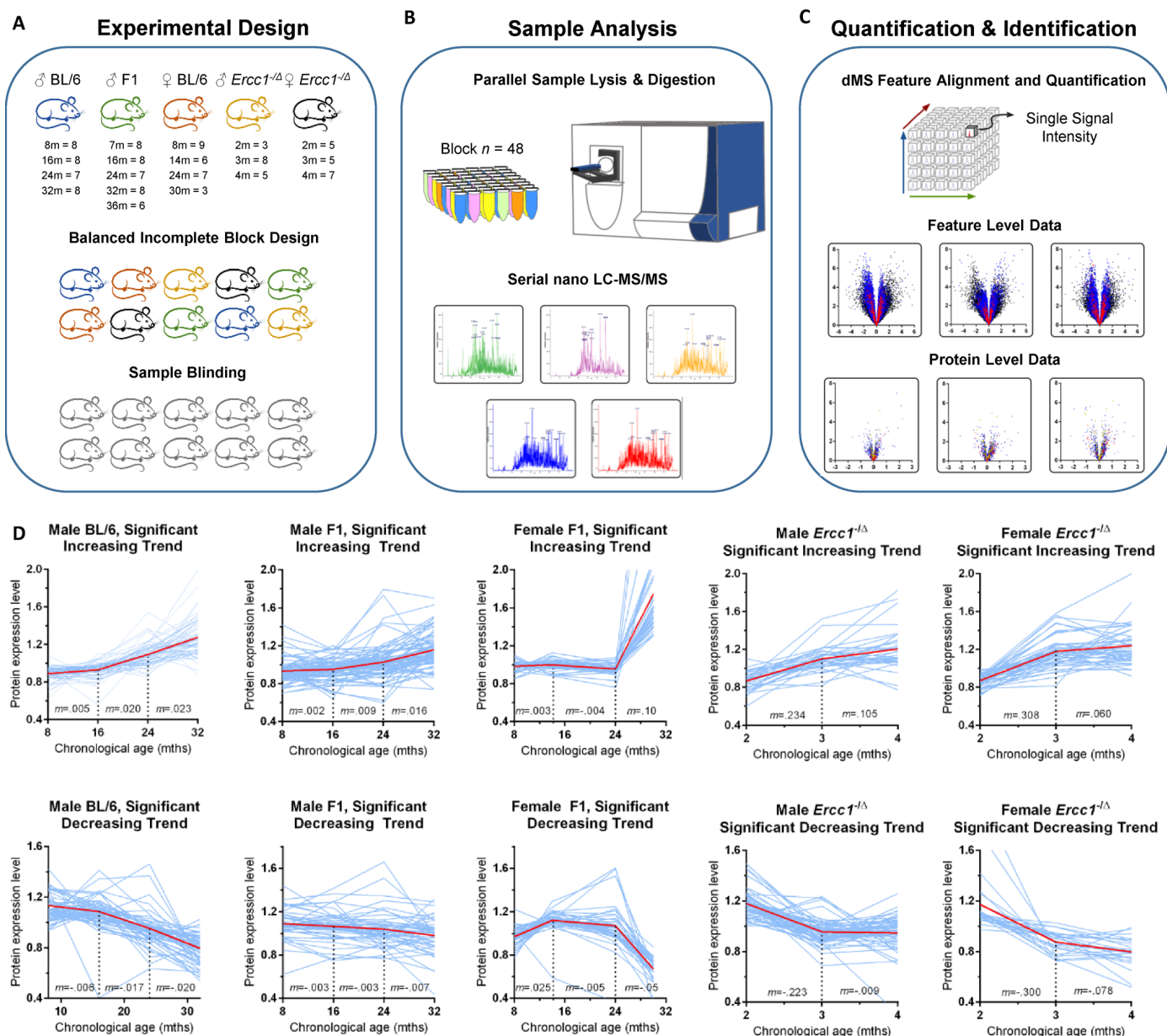


**Figure 1. Unbiased detection of age-related changes in protein expression in mouse liver.** (A) Details of input tissue samples (age in months and  $n$  per group) and methods of bias mitigation for sample preparation and analysis, including the creation of a balanced incomplete block design for all processing and analysis steps and sample blinding. For the *Ercc1*<sup>-Δ</sup> mouse liver the  $n$  refers to mutant mice / littermate controls. (B) Sample processing block size and representative mass chromatograms generated from each sample. See methods section for more detail. (C) Alignment, extraction, and storage of mass spectral feature data from raw mass spectrometer output based on retention time and accurate mass, allowing for quantification of each proteomic signal across all samples, results of which are shown in example feature level volcano plots. The y-axis is the negative log of  $p$ -value; the x-axis is the log fold-change in protein abundance. All features associated with a protein are combined to calculate protein expression as shown in volcano plots indicating proteins (individual dots) that were significantly increased or decreased in expression in old vs. young mice and the extent of that change in expression. (D) Plots of the relative abundance of all proteins (individual blue lines) that change significantly with aging as identified by one-way ANOVA. Protein expression was measured cross-sectionally throughout the lifespan of inbred male C57BL/6Jnia, male f1a (C57BL/6Jnia:Balb/cBy), female f1b (C57BL/6J:FVB/NJ), male f1b (C57BL/6J:FVB/NJ) *Ercc1*<sup>-Δ</sup>, and female f1b (C57BL/6J:FVB/NJ) *Ercc1*<sup>-Δ</sup> mouse livers. The graphs are separated into proteins that increased in expression with chronological age (top) or decreased (bottom). The red line represents the mean protein abundance for significantly altered proteins in that group.  $m$  = the slope between time points. Significance cutoffs as delineated in Supplementary Table 2.

In inbred male mice, 64,657 features passed occupancy and outlier filtering, which led to a total of 34,817 features quantified and identified with high precision. Tandem mass spectrometry data was used to link these features to 7,962 peptides that are uniquely found in 1,298 protein sequences. Detailed numbers of features and proteins quantified for each strain of mice is provided in Supplementary Table 2. Supplementary Tables 3-5 list the proteins for each of the strains of WT mice that met the minimum significance cutoff of <5% false discovery based on iterative random sampling strategy [15]. Differences in protein expression between age groups of mice was small (<20%) for the majority of proteins.

Line plots of relative protein abundance as a function of chronological age are shown for proteins that exhibited a significant increase or decrease with age (Figure 1D). Interestingly, the age when the most dramatic inflection in expression levels occurred is identical for over- and under-expressed proteins for a given mouse strain. But the age at greatest inflection in protein expression differed substantially between strains of mice. For example, in inbred male mice, protein expression is stable from 8-16 months of age then changes more dramatically between 16-24 and 24-32 months of age. In the longer-lived f1a male and f1b female mice, protein expression was stable into the third age group (24 months of age). After that (from 24 to 32 months), changes in protein abundance were more dramatic. This was particularly true in female mice, which is consistent with data indicating that several measures of health (body weight, percent fat mass and grip strength) drop more precipitously in female mice towards the end of life, whereas male mice experience a more steady decline in the last 12-16 months of life [16]. By analogy, women have a longer lifespan than men yet have greater disability and poorer health in old age [17].

Although not the main focus of this work, pathway enrichment mining was performed using the proteomic data from the oldest and youngest age groups for the three strains of wild-type mice (Supplementary Table 6). There was remarkable consistency in age-related protein expression levels between the three strains (inbred, f1a and f1b) of WT mice, even at the level of individual proteins. The pathways most significantly altered were oxidative damage/antioxidant response, fatty acid oxidation, nuclear receptors and clathrin-mediated endocytosis. Expression of proteins required for fatty acid oxidation was significantly reduced in liver of older mice compared to the younger age groups (Supplementary Figures 2 and 3) consistent with prior studies [18] and evidence that aged WT mice have fatty liver compared to younger adult animals (Supplementary Figure 2B). In contrast, expression of proteins

related to endocytosis and phagocytosis were significantly increased with aging (Supplementary Figures 4 and 5).

To determine if it is possible to define a signature of age-related changes from the unbiased data set, a subset of the 1,298 proteins quantified in inbred male mice were selected based on high sample occupancy, strong statistical significance, and low intra-individual variance (Figure 2A). The Jonckheere-Terstra ordinal trend test and the Kruskal-Wallis test were used to evaluate protein expression trends between samples (Supplementary Table 15) [19, 20]. This yielded a panel of 14 proteins that were used to “set a biological clock” by which to gauge the aging of other mouse strains relative to C57BL/6Jnia inbred mice. A rudimentary linear model that weighted each of the 14 proteins equally was used to define the protein expression profile at 16, 24, and 32 months of age in a reference population of inbred mice (Supplementary Table 14). Thereby in C57BL/6 mice, chronological age was equated with biological age to create a frame of reference.

Expression of 11 of the 14 panel proteins differed between male f1a and male C57BL/6 mice, often at multiple time points, *i.e.*, multiple ages (Figure 2B). Notably, in all cases where there were differences between strains, if the expression declined with aging in inbred mice, this effect was blunted in the f1a mice, consistent with slower biological aging (Figure 2B). For example, the expression of carbonic anhydrase 3 (CA3) was observed to decrease dramatically with aging in C57BL/6 mice, but less dramatically in f1a mice (Figure 2B and Supplementary Table 3). Immunoblot detection of CA3 confirmed decreased expression in liver of 24 month-old inbred mice compared to age-matched f1a mice, consistent with the dMS data (Figure 2C).

Summation of the differences in expression of the 14 selected proteins enabled calculation of the biological age of f1a male mice relative to the inbred males (Figure 2D; see methods for details). We anticipated that the f1a male mice, which are known to be healthier and longer-lived [21-23] would have a younger “biological age” than chronologically age-matched inbred mice. Indeed, 24 month-old f1a mice appeared 16 months-old on the reference scale ( $p<0.001$ ). 32 month-old f1a mice appeared 24 months-old ( $p<0.0001$ ). Thus, by comparison to inbred mice, the f1 hybrid mice were calculated to be significantly younger biologically than their chronologic age.

These proteomic results were supported by pre-mortem functional data and post-mortem histopathologic analy-



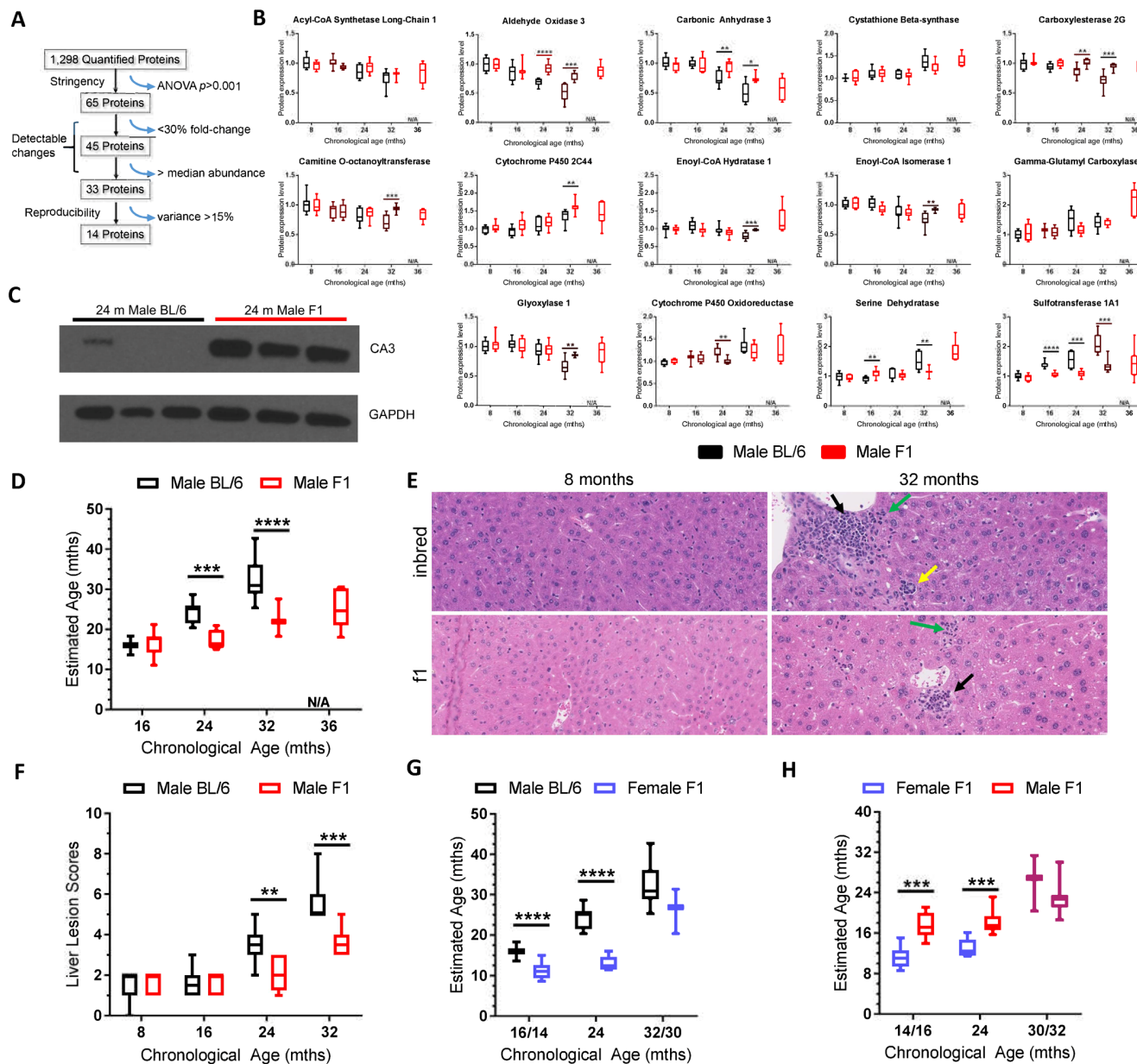


**Figure 2. Selection of the biological age calculator protein panel and its application to other strains of wild-type mice.** (A) Illustration of how the 14 protein panel was selected from the 1,298 proteins that were quantified in liver of C57BL/6Jnia mice. 65 proteins had a one-way ANOVA  $p < 0.001$ , providing high statistical significance in age-related changes in expression. 45 of those proteins had a fold-change difference of  $\geq 30\%$  and 33 of those had abundance above the median, facilitating detection of expression changes. 14 of those 33 proteins had a maximal intragroup variance of 15%, supporting reproducibility. (B) Expression of the 14 proteins selected for the biological age calculator in male C57BL/6J mouse liver (black) and male f1a mouse liver (red) at multiple ages. (C) Immunoblot detection of carbonic anhydrase 3 expression in liver from three 24 month-old inbred and three f1a mice. The tissue lysates used were the same as those used in the MS experiments, providing intra-experimental validation. (D) The combined expression data from the panel of 14 proteins sets the biological (estimated) age to the chronological age for the reference group of mice, C57BL/6Jnia (i.e., the black bars define 16, 24 and 32 months according to the biological age calculator; see methods for more details). Red bars represent the summation of the data on the same 14 proteins in male f1a mice estimating their biological age at the chronological ages of 8, 16, 24, and 32 months relative to the reference strain. (E) Representative images of liver sections from male inbred (C57BL/6Jnia) and f1a (C57BL6/Jnia:Balb/cBy) mice at two ages. The older mice show numerous age-related lesions consisting of portal inflammation (green arrows), portal duct hyperplasia (yellow), microgranulomas (black) and mild intermittent hepatic degeneration. The inbred mice had more extensive age-related lesions than the f1a mice. (F) The composite lesion score reflects the incidence and severity of a specific panel of age-related liver lesions and was used as a separate calculator of biological age, in the same C57BL/6Jnia (black) and f1a (red) male mice used for proteomic analysis. (G) Same as (D) but for female mice of a different f1b strain (blue). The female mice were analyzed at 14 rather than 16 months of age and 30 vs. 32 months of age (x-axis). (H) Estimated biological age of f1b female (blue) vs. f1a male mice (red). Significance testing for all panels using Student's unpaired, equal variance t-test, error bars show SEM. \* $p < 0.05$ , \*\* $p < 0.01$ , \*\*\* $p < 0.001$ , \*\*\*\* $p < 0.0001$ ; N/A, not applicable.

sis from the exact same mice as those used in the proteomics analysis. The fl<sub>a</sub> mice had significantly greater mean distance traveled in a voluntary running wheel at all ages, than did the inbred mice [24]. The fl<sub>a</sub> mice also maintained VO<sub>2</sub> or energy expenditure into old age, unlike the inbred mice, which displayed a significant drop in VO<sub>2</sub> in the eldest age group (Supplementary Table 7). These data are consistent with the fl<sub>a</sub> male mice being biologically younger than the inbred mice.

Post-mortem histopathologic analysis of liver revealed increased age-related histopathological lesions in the C57BL/6Jnia mice compared to that of age-matched fl<sub>a</sub> mice (Figure 2E). The composite lesion score (CLS) for a defined set of age-related liver lesions [25] was significantly lower in 24 and 32 month-old fl<sub>a</sub> mice compared to the inbred mice (Figure 2F). Analogous to the protein expression data (Figures 1D and 2B), the CLS for male C57BL/6Jnia mice was unchanged between 8 and 16 months, before increasing linearly between 16 and 32 months. In contrast, CLS for the male fl<sub>a</sub> mice was unchanged until 24 months of age. At 32 months, the fl<sub>a</sub> CLS was equal to that of the 24 month-old inbred mice. Thus, histopathologic analysis of liver is consistent with the proteomics data.

The total CLS derived from histopathologic analysis of four organs (heart, lung, kidney and liver) of the mice used for proteomics analysis was significantly lower in 24 and 32-month-old fl<sub>a</sub> mice compared to inbred mice (Supplementary Table 8), as were the organ-specific CLS for 3 of the 4 organs examined (Supplementary Table 9) supporting the conclusion that the two strains of mice age at different rates. This independent method of determining biological age was entirely consistent with the proteomics-based biological age calculator. Thus, both pre-mortem and post-mortem analysis of the mice used in the initial proteomics analysis indicate that the fl<sub>a</sub> mice are biologically younger than chronologically age-matched inbred mice, as the dMS proteomics analysis predicted.

Based on the 14 signature proteins (Supplementary Figure 6), female mice in a distinct genetic background (called fl<sub>b</sub>) also were significantly biologically younger than the reference inbred male mice throughout the first two years of life (Figure 2G). At 14 and 24 months of age, the females were predicted to be 10 and 13 months-old, respectively. But by 30 months of age, their predicted biological age was roughly equivalent to their chronological age, consistent with the slopes of the trend plots shown in Figure 1D. This was recapitulated by comparing the female fl<sub>b</sub> and male fl<sub>a</sub> mice (Figure 2H), where female mice were calculated to be significantly younger than male mice through the first two

years of life. But the sex-specific differences were absent by 30-32 months of age. This sex-specific differences in pace of aging is supported by the observation that expression of two markers of cellular senescence (*p16<sup>Ink4a</sup>* and *p21<sup>Cip1</sup>*), a well-recognized driver of aging [26, 27], was significantly greater in liver tissue of male fl<sub>b</sub> than female fl<sub>b</sub> mice at 24 months of age, but the sex differences were all but lost by 32 months of age (Supplementary Figure 7).

The liver proteomics data from mice of both sexes and two genetic backgrounds compared to the reference inbred C57BL/6Jnia mice provides two examples where the profile of liver protein expression obtained by dMS predicted differences in the biological age between the groups of mice. This prediction was supported by our functional and histopathological data as well as prior studies indicating that fl<sub>a</sub> mice have a longer lifespan than inbred animals [21, 22].

To further challenge the utility of the biological age calculator, we used genetic and pharmacologic approaches to accelerate and decelerate aging. *Ercc1<sup>-Δ</sup>* mice model a human progeroid syndrome [28], aging rapidly between 2-6 months of life [29]. Liver from 2, 3, and 4 month-old *Ercc1<sup>-Δ</sup>* mice was compared to age-matched WT mice, both in an fl<sub>b</sub> genetic background, using dMS. This yielded >1,000 proteins that were differentially expressed between the progeroid and WT mice (Supplementary Tables 1, 2, 10 and 11). Plotting the expression of all of the proteins that were altered with aging in the *Ercc1<sup>-Δ</sup>* mouse liver revealed an inflection point at 3 months of age for both male and female mice (Figure 1D). The differences in protein expression between progeroid and WT mice rose more quickly between 2-3 months of age than between 3-4 months.

The expression level of 11 of the 14 panel proteins was significantly different between male *Ercc1<sup>-Δ</sup>* mice and age-matched WT congenic male mice (Figure 3A). For 8 of these 11 proteins, the differences in expression between *Ercc1<sup>-Δ</sup>* mice and age-matched WT mice was in the same direction as aging-related changes in WT mice, *i.e.*, if protein expression went down with aging in WT mice, it was lower in *Ercc1<sup>-Δ</sup>* mice compared to age-matched WT controls. Across the lifespan of the *Ercc1<sup>-Δ</sup>* mice, protein expression tended to trend in the same direction as what occurred with normal aging for all 14 proteins (at least from 2-3 months of age). Furthermore, as the mutant mice aged from 2-4 months, protein expression differed significantly from that in age-matched WT mice ( $p < 0.001$  for both sexes). Immunoblot detection confirmed decreased levels of CA3 in progeroid *Ercc1<sup>-Δ</sup>* mice compared to age-matched WT mice (Figure 3B).

























